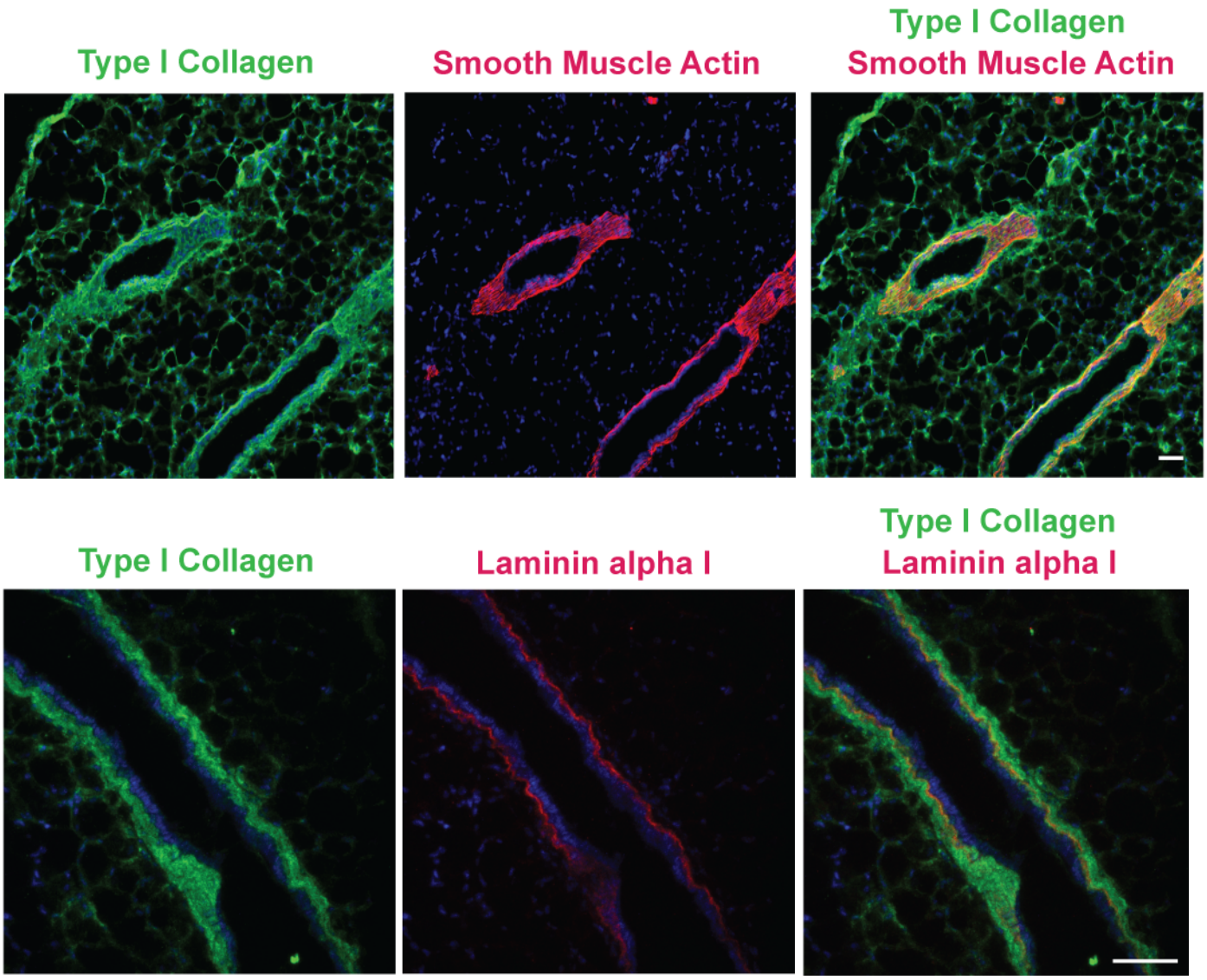

Fig. S1. Mammary epithelial cells in vivo are surrounded by type I collagen. The MG from virgin C57BL/6 mouse at 8 weeks was cryosectioned and stained for type I collagen (upper and lower panels; green), α-smooth muscle actin (upper panels; red) and laminin α1 (lower panels; red). Type I collagen is present in basement membrane that surrounds the mammary ducts. Anti-type I collagen (Chemicon), anti-α-smooth muscle actin (Sigma) and anti-laminin α1 (a kind gift from Dr Srorokin, University of Münster, Germany) were used as primary antibodies, and fluorescence conjugated goat anti-mouse IgG or anti-rabbit IgG (Invitrogen) were used for visualizing images. All images were captured by confocal microscopy (Solamere Technology Group). Scale bar: 100 μm.

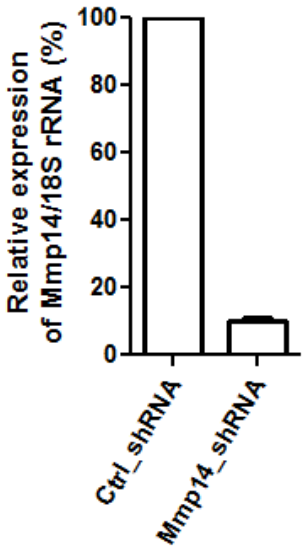

Fig. S2. Quantitative RT-PCR analysis of *Mmp14*- silenced EpH4 cells. Quantitative RT-PCR was performed to confirm a loss *Mmp14* expression in *Mmp14*-silenced EpH4 cells. n=3. Data are mean±s.e.m. P<0.001.

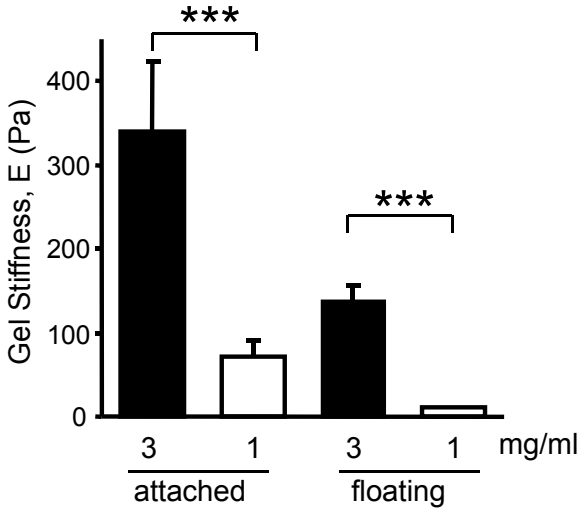

Fig. S3. Atomic force microscopy measurements confirmed the physiological collagen density and stiffness in 3D CL-1 gels. Atomic force microscopy analysis of dense (3 mg/ml) and sparse (1 mg/ml) CL-1 gel stiffness for attached and floating CL-1 gels. Data are mean±s.e.m. ***P<0.001.

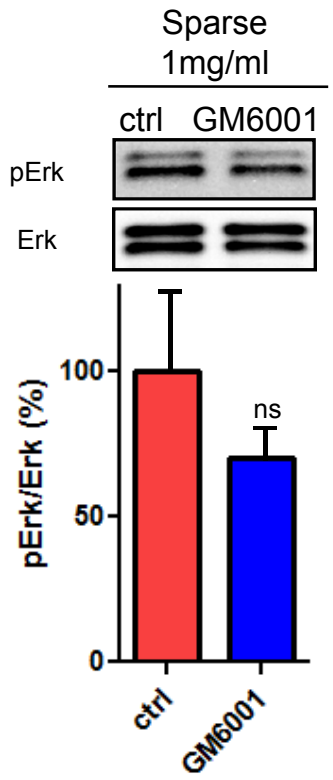

Fig. S4. Metalloproteinase activity is not required for Erk1/2 phosphorylation in collagen 1-coated gels. EpH4 cells were cultured in collagen for 24 hours with or without GM6001 (40 μM). Ratio between pErk and total Erk is indicated. Values were normalized to Erk activity of ctrl-treated EpH4 cells in sparse collagen, n=3. NS indicates no significance, as measured by two-tailed t-test.

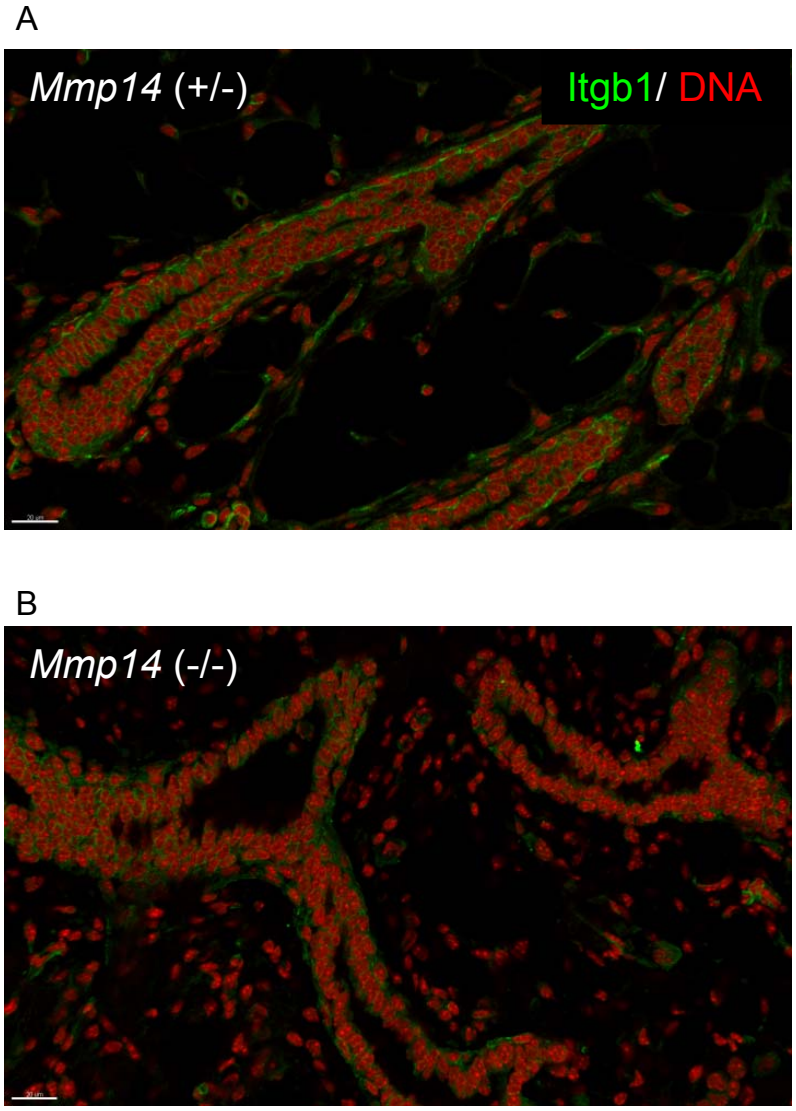

Fig. S5. The mammary glands of *Mmp14*$^{-/-}$ mice have lower Itgb1 expression levels. MGs from (**A**) *Mmp14*$^{+/-}$ or (**B**) *Mmp14*$^{-/-}$ mice were immunostained for Itgb1 (green) and with DAPI (red). See Fig. 3Aiv for quantification of Itgb1 intensity. The mammary gland from *Mmp14*$^{-/-}$ mice showed fewer lipid droplets in the mammary fat tissue. This phenotype might be due to less adipogenesis as reported previously (Chun et al., 2006).

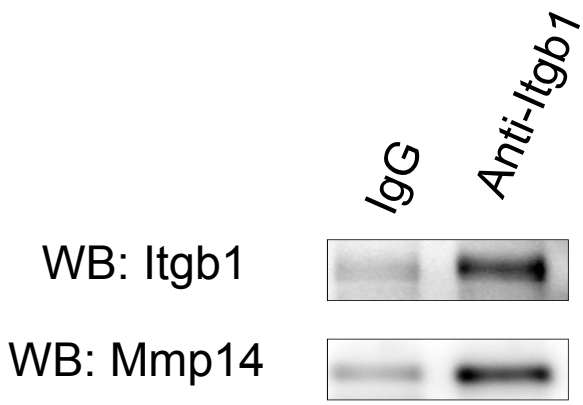

Fig. S6. Immunoprecipitation of Itgb1 detects Mmp14. Endogenous Itgb1 was immunoprecipitated with hamster anti-Itgb1 (Santa Cruz Biotechnology) from the EpH4 cell lysate. Immunoprecipitated material was probed for Itgb1 and Mmp14 using rabbit anti-Itgb1 (Santa Cruz Biotechnology) or rabbit anti-Mmp14 (Abcam), respectively. Control hamster IgG was purchased from Santa Cruz Biotechnology.

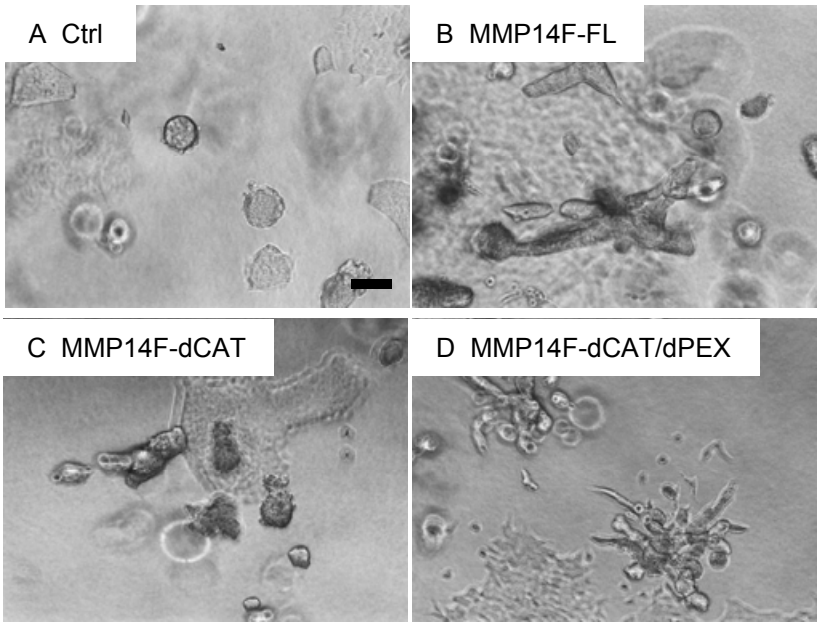

Fig. S7. Overexpressing full-length MMP14 or the dCAT/dPEX mutant in *Mmp14*-silenced EpH4 cells rescues MEC invasion/branching in sparse CL-1 gels. *Mmp14*-silenced EpH4 cells were infected with lentivirus containing (**A**) control, (**B**) *MMP14F-FL*, (**C**) *MMP14F-dCAT* or (**D**) *MMP14F-dCAT/dPEX,* respectively. Cells were cultured in 1 mg/ml CL-1-coated gel. Scale bar: 100 μm.

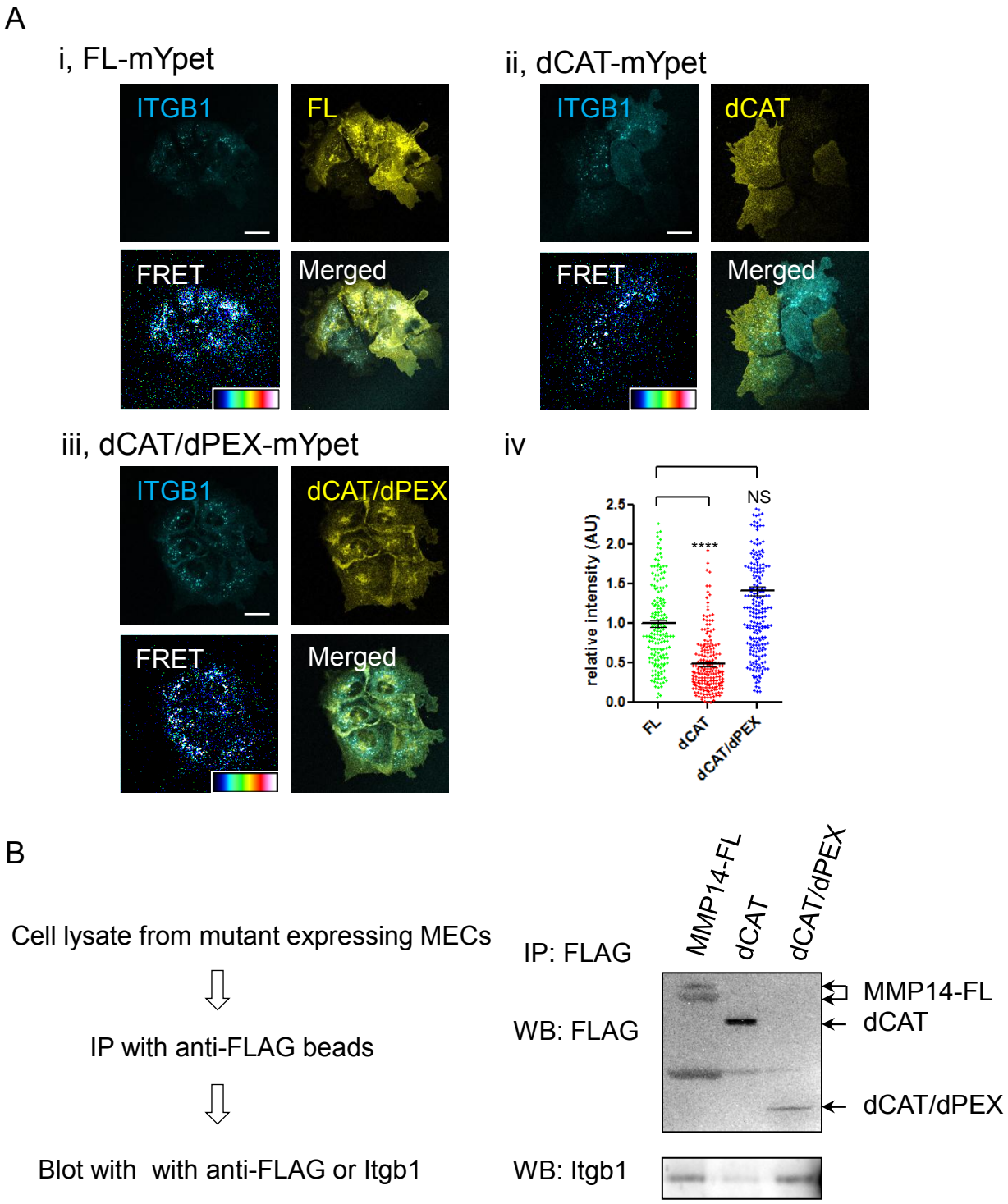

Fig. S8. MMP14-FL and MMP14-dCAT/dPEX associate with Itgb1, but MMP14dCAT does not. (**A**) FRET analysis was performed on Mmp14-silenced EpH4 cells. ITGB1 mCypet was expressed as a FRET donor and mYpet tagged MMP14 mutants were used as a FRET acceptor. Ypet emission signal was detected when Cypet was excited, indicating FRET. (i) ITGB1mCypet/MMP14 FL-mYpet, (ii) ITGB1mCypet/dCAT-mYpet and (iii) ITGB1mCypet/dCAT dPEX-mYpet were shown. The heat map indicator is presented to show the intensity of the FRET signal. (iv) Quantification of FRET signals. Approximately 200 FRET signals were quantified on each condition. Data are mean±s.e.m. ****P<0.001. (**B**) Immunoprecipitation between MMP14 mutants and Itgb1. MMP14-FL, dCAT or dCAT/dPEX expressing EpH4 cells were lysed with lysis buffer (1% Brij98, 25 mM HEPES pH 7.4, 150 mM NaCl, protease inhibitors), and immunoprecipitated with anti-FLAG M2 beads (Sigma). Immunocomplexes are used for IP-WB analysis. Blots show FLAG tagged MMP14 mutants (upper) and Itgb1 (lower).

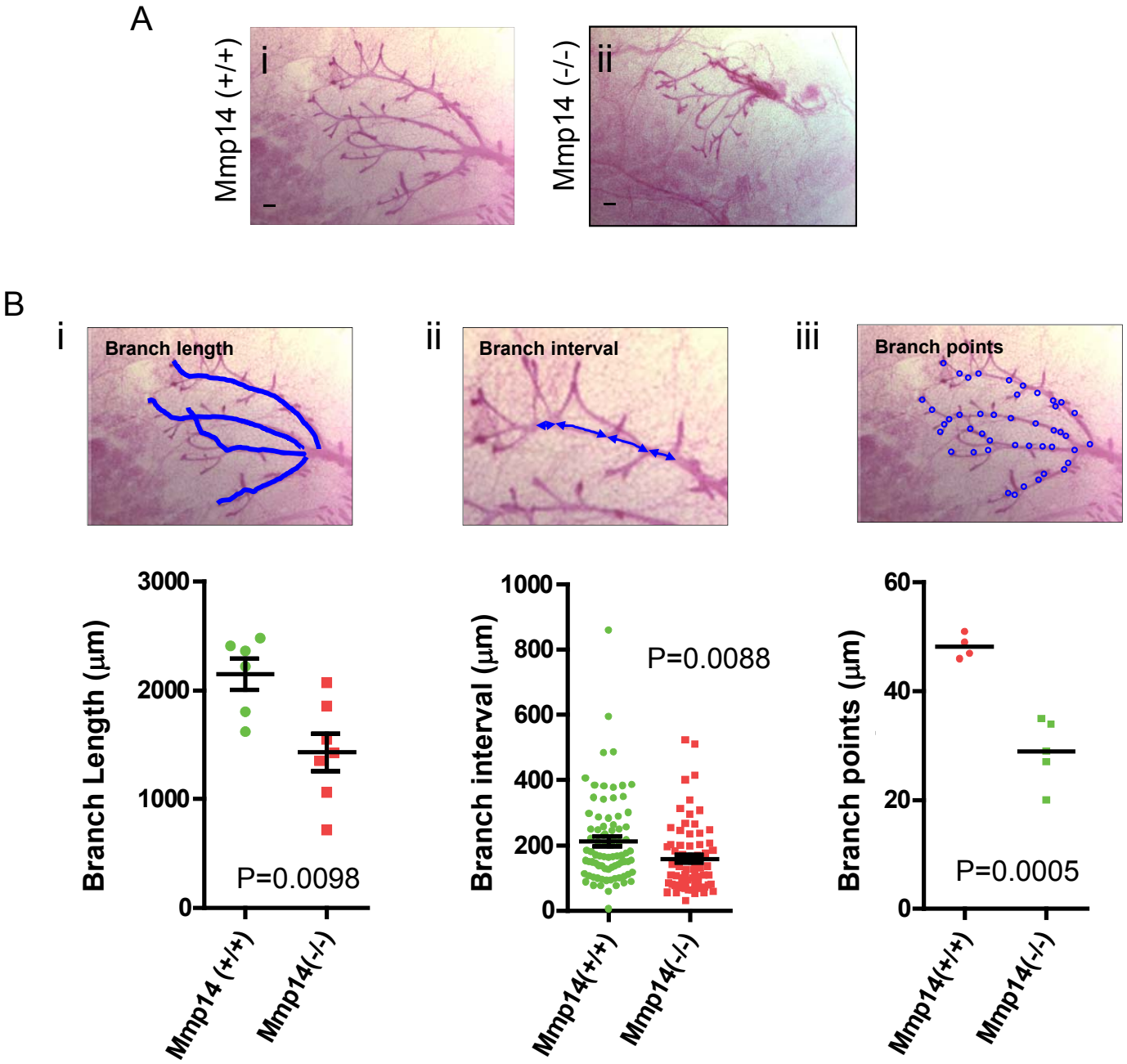

Fig. S9. Mammary gland branching morphogenesis is reduced in *Mmp14*$^{-/-}$ mouse. (**A**) The ductal tree in the mammary gland from (i) wild-type and (ii) *Mmp14*KO are shown. Tissue images were captured with confocal microscopy to quantify 3D parameters (Mori et al., 2012). (**B**) Branch length (i), branch interval (ii) and branch points (iii) were analyzed with IMARIS software (Bitplane). *n*=5. Scale bar: 200 μm.

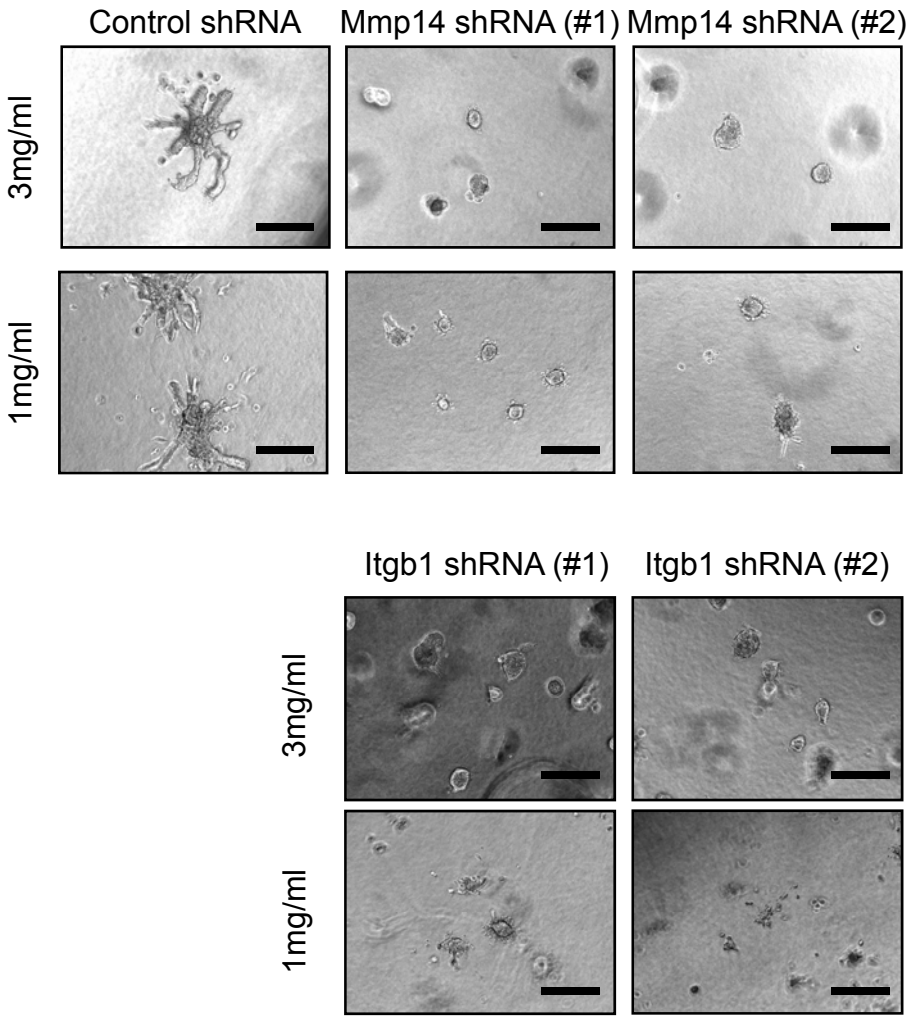

Mmp14 hairpin sequences
#1, CCGGCCATCAATACTGCCTACGAAACTCGAGTTTCGTAGGCAGTATTGATGGTTTTTG
#2, CCGGGCAGTGATGAAGTCTTCACATCTCGAGATGTGAAGACTTCATCACTGCTTTTTG
#3, CCGGCCAGCAACTTTATGGAAGCAACTCGAGTTGCTTCCATAAAGTTGCTGGTTTTTG
#4, CCGGCGGATAAGTTTGGGACTGAGACTCGAGTCTCAGTCCCAAACTTATCCGTTTTTG

Itgb1 hairpin sequences
#1, CCGGCCAAGTTTCAAGGGCCAACTTCTCGAGAAGTTGGCCCTTGAAACTTGGTTTTTG
#2, CCGGCCCGACATCATCCCAATTGTACTCGAGTACAATTGGGATGATGTCGGGTTTTTG
#3, CCGGGCCATTACTATGATTATCCTTCTCGAGAAGGATAATCATAGTAATGGCTTTTTG
#4, CCGGGCACGATGTGATGATTTAGAACTCGAGTTCTAAATCATCACATCGTGCTTTTTG

Fig. S10. Invasion/branching is inhibited by silencing either Mmp14 or Itgb1 in CL-1 gels. Images show *Mmp14*- or *Itgb1*-silenced EpH4 cells in dense (3 mg/ml) or sparse (1 mg/ml) CL-1-coated gels. Short hairpin sequences for Mmp14 or Itgb1 are indicated below. Total RNA was isolated from shRNA-treated MECs, and tested to validate knock down. Sequences 1 and 2 on the list provided more than an 80% knock down and were used in experiments. The short hairpin sequences for Mmp14 and Itgb1 are indicated.